OFFICE OF NAVAL RESEARCH

Contract N00014-79-C-0647

TECHNICAL REPORT #55

Monte Carlo Simulations of Small Solute/Solvent Clusters: Cluster Properties and Phase Transitions

by

S. Li and E. R. Bernstein

Prepared for Publication

in the

Journal of Chemical Physics

Department of Chemistry
Colorado State University
Fort Collins, Colorado 80523

June 1, 1989

SECURITY CLASSIFICATION OF THIS PAGE

REPORT DOCUMENTATION PAGE

Form Approved
OMB No 0704-0188

1a REPORT SECURITY CLASSIFICATION	1b RESTRICTIVE MARKINGS
2a SECURITY CLASSIFICATION AUTHORITY	3 DISTRIBUTION / AVAILABILITY OF REPORT Aporoved for public release; distribution unlimited.
2b DECLASSIFICATION / DOWNGRADING SCHEDULE Unclassified	
4 PERFORMING ORGANIZATION REPORT NUMBER(S) N00014-79-C-0647	5 MONITORING ORGANIZATION REPORT NUMBER(S)
6a NAME OF PERFORMING ORGANIZATION Colorado State University 6b OFFICE SYMBOL (If applicable)	7a NAME OF MONITORING ORGANIZATION
6c ADDRESS (City, State, and ZIP Code) Department of Chemistry Fort Collins, CO 80523	7b ADDRESS (City, State, and ZIP Code)
8a NAME OF FUNDING / SPONSORING ORGANIZATION Office of Naval Research 8b OFFICE SYMBOL (If applicable)	9 PROCUREMENT INSTRUMENT IDENTIFICATION NUMBER N00014-79-C-0647
8c ADDRESS (City, State, and ZIP Code) 800 North Quincy Street Arlington, VA 22217-5000	10 SOURCE OF FUNDING NUMBERS PROGRAM ELEMENT NO / PROJECT NO / TASK NO / WORK UNIT ACCESSION NO

11 TITLE (Include Security Classification)
"Monte Carlo Simulations of Small Solute/Solvent Clusters: Cluster Properties and Phase Transitions"

12 PERSONAL AUTHOR(S)
S. Li and E. R. Bernstein

13a TYPE OF REPORT	13b TIME COVERED	14 DATE OF REPORT (Year, Month, Day)	15 PAGE COUNT
Technical Report	FROM _____ TO _____	June 1, 1989	

16 SUPPLEMENTARY NOTATION

17 COSATI CODES			18 SUBJECT TERMS (Continue on reverse if necessary and identify by block number)
FIELD	GROUP	SUB-GROUP	Monte Carlo calculations, clusters, phase transitions, nucleation of clusters, cluster properties, temperature dependence.

19 ABSTRACT (Continue on reverse if necessary and identify by block number)

SEE ATTACHED ABSTRACT

20 DISTRIBUTION / AVAILABILITY OF ABSTRACT	21 ABSTRACT SECURITY CLASSIFICATION
☒ UNCLASSIFIED/UNLIMITED ☐ SAME AS RPT ☐ DTIC USERS	Unclassified
22a NAME OF RESPONSIBLE INDIVIDUAL Elliot R. Bernstein	22b TELEPHONE (Include Area Code) (303) 491-6347
	22c OFFICE SYMBOL

DD Form 1473, JUN 86 Previous editions are obsolete SECURITY CLASSIFICATION OF THIS PAGE

S/N 0102-LF-014-6603

Abstract

Atom-atom L-J (6-12-1) potentials are employed to calculate the cluster configurations of all local energy minima of benzene$(N_2)_n$ and $(N_2)_n$ clusters for n=1, 2,.....10 and some benzene$(Ar)_n$ and $N_2(Ar)_n$ clusters. The number of configurations increases exponentially and the binding energy range increases linearly with the number of solvent molecules for these clusters. Monte Carlo simulations are performed on the temperature behavior of the cluster potential energy, intermolecular distance, and some angular variables for benzene$(Ar)_n$ and benzene$(N_2)_n$ clusters.

Molecules comprising the cluster can undergo tunneling between the different potential energy minima at particular transition temperatures. This tunneling process can be viewed as a solid-solid or solid-liquid phase transition for the cluster.

Cluster properties vary smoothly with temperature if the temperature remains below the transition temperature. If an interpotential well tunneling occurs for molecules in a given cluster, a thermodynamic property or a proper order parameter can always be found which detects the tunneling in the cluster. A rapid molecular tunneling between various potential energy minima is indicative of the liquid phase. As in the bulk, not all system variables evidence this phase transition behavior with equal clarity or even equal intensity. Knowledge of cluster structure is therefore directly related to the understanding of cluster phase transitions.

MONTE CARLO SIMULATIONS OF SMALL SOLUTE/SOLVENT CLUSTERS: CLUSTER PROPERTIES AND PHASE TRANSITIONS+

S. Li and E. R. Bernstein

Chemistry Department
Colorado State University
Fort Collins, Colorado 80523

+ Supported in part by a grant from the Office of Naval Research

Abstract

Atom-atom L-J (6-12-1) potentials are employed to calculate the cluster configurations of all local energy minima of benzene$(N_2)_n$ and $(N_2)_n$ clusters for n=1, 2,.....10 and some benzene$(Ar)_n$ and $N_2(Ar)_n$ clusters. The number of configurations increases exponentially and the binding energy range increases linearly with the number of solvent molecules for these clusters. Monte Carlo simulations are performed on the temperature behavior of the cluster potential energy, intermolecular distance, and some angular variables for benzene$(Ar)_n$, and benzene$(N_2)_n$ clusters.

Molecules comprising the cluster can undergo tunneling between the different potential energy minima at particular transition temperatures. This tunneling process can be viewed as a solid-solid or solid-liquid phase transition for the cluster.

Cluster properties vary smoothly with temperature if the temperature remains below the transition temperature. If an interpotential well tunneling occurs for molecules in a given cluster, a thermodynamic property or a proper order parameter can always be found which detects the tunneling in the cluster. A rapid molecular tunneling between various potential energy minima is indicative of the liquid phase. As in the bulk, not all system variables evidence this phase transition behavior with equal clarity or even equal intensity. Knowledge of cluster structure is therefore directly related to the understanding of cluster phase transitions.

I. INTRODUCTION

The properties and behavior of small clusters are of considerable practical and theoretical interest due to their importance for aerosol formation, atmospheric chemistry, crystal growth and nucleation theory. The thermodynamics and dynamics of small clusters of Lennard-Jones (L-J) atoms have been studied by both molecular dynamics (MD)[1-3] and Monte Carlo (MC)[4-12] simulations. These two calculational algorithms take slightly different approaches to the cluster ensemble thermodynamics and dynamics: MC calculations fix temperature and obtain the cluster intermolecular potential energy, simulating a canonical ensemble; MD calculations fix the total energy for the cluster ensemble and obtain the system temperature from the cluster kinetic energy, simulating a micro-canonical ensemble. Most of the model systems studied are applicable to homogeneous nucleation and are specific to argon clusters of different sizes: inhomogeneous systems and clusters of constant size but different configurations have not received a great deal of attention.[5]

The melting, freezing and dissociation behavior of small clusters plays a central role in bulk phase transitions. Cluster (microcrystal) formation and disintegration are the predecessors to phase transitions. Both MD[1-3] and MC[9-12] studies of the melting and freezing of small L-J clusters have been reported. MC calculations[9-11] suggest solid-liquid phase transitions for clusters of n = 3 to 13 argon atoms. MD calculations generate similar results for as few as seven argon atoms and suggest a liquid-solid coexistence region for argon clusters.[2-3] The coexistence of liquid and solid clusters seems to arise theoretically in both classical and quantum mechanical calculations.[13-14] Both liquid-like and solid-like clusters are suggested to be present in supersonic expansions[15-16], although multiple cluster configurations may also give rise to similar observations.

Our present efforts deal with modeling the inhomogeneous nucleation process. This paper reports information concerning this process obtained from computer MC modeling of clustering. We consider the general topics of cluster configuration, internal energy and phase transitions. For each of these general topics we address specific issues as follows:

Cluster configuration - 1. number of distinct configurations as a function of cluster components, 2. temperature evolution of each configuration, 3. relation of cluster configuration to cluster phase behavior.

Cluster internal energy - 1. relation between binding energy, binding energy/molecule and cluster size, 2. behavior of potential energy as a function of temperature, 3. relation between cluster phase behavior and cluster potential energy.

Phase transitions - 1. structure and property changes at phase transitions, 2. phase coexistence in single clusters and cluster ensembles, 3. order parameters for cluster phase transitions.

In the current report we focus attention on small ($n \leq 10$) clusters of nitrogen, argon and benzene/nitrogen and argon.

II. SIMULATION METHODS

Cluster internal energy minimization and MC simulation procedures employ atom-atom L-J (6-12-1) potentials[17] in the form

$$U_{ij} = A_{ij}/r_{ij}^{12} - C_{ij}/r_{ij}^{6} + e_i e_j/r_{ij} \qquad (1)$$

in which parameters A_{ij}, C_{ij} are given in Table I for interactions of the same atoms, r_{ij} is the interatomic distance between atoms i and j on different molecules, and e_i is the partial charge on atom i. Partial atomic charges are adapted from ref. 18 and 19 and MOPAC 5 calculations[20]. Potential constants for unlike interacting atoms are treated according to ref. 17.

Starting configurations for the energy minimization procedure for two component clusters are generated randomly. The energy minimization routine employs golden section searching and conjugate gradient algorithms to reduce computational time.[21] The computation ensures that molecules translate and rotate toward structures of lower energy, that molecules are eventually trapped in energy minima and that after numerous simulations all possible potential energy minima on the potential energy surface are located. The cluster binding energy thus obtained for a particular cluster configuration (e.g, $C_6H_6(N_2)_n$, n=1, . . . , 13)

can be viewed as the proper statistical average energy for that cluster at O K.

Cluster potential energies, configurations and properties are calculated at non-zero temperatures through MC calculations: millions of steps at each temperature for each O K cluster configuration are required. As the temperature is increased in these simulations, both the number of simulation steps and the step size also increase in order to maintain accurate results. Radial, energy and angular distributions are recorded at each temperature for each cluster structure. The time (MC step) dependence of the intermolecular distances, angles, and potential energy, along with their standard deviations, are also recorded at each temperature. MC simulations for $C_6H_6(N_2)_n$ n=1, . . . 6 clusters have been carried out and their results are reported in the next section.

Tunneling between different solid-like cluster configurations occurs as the temperature is increased in an MC simulation. Such tunneling has, in some instances, been prohibited in order to obtain the temperature dependence of the cluster potential energy for each distinct cluster configuration over a large temperature range.

The solid-gas and liquid-gas phase behavior of these clusters is not well characterized with regard to transition temperature because the simulation assumes an infinite volume for the clustering system. The solid-liquid transition and any phase "coexistence ranges" will also not have an accurate temperature behavior. In order to portray these dynamics accurately with temperature in an MC simulation, large ensembles of clusters should be simulated; alternatively one cluster must undergo the transition numerous times and the amount of time the cluster spends in each phase must be monitored.

A number of bulk phase concepts are useful in discussing cluster properties and behavior (e.g., phase transitions, phases, crystal, liquid, glass); however, in clusters these concepts do not have rigorous definitions. For example, phase transition behavior in bulk materials is typically characterized by discontinuities in thermodynamic properties or their derivatives, but no such rigorous definitions are possible for small clusters.

We will refer to the cluster binding energy as the O K potential energy of the system; a configuration of a cluster is a geometry of molecules for which a local binding energy minimum has been achieved.

III. OBSERVATIONS FROM COMPUTER SIMULATIONS

The number of cluster configurations for a fixed composition cluster increases dramatically with cluster size. Figure 1 presents the number of configurations with different energies as a function of the number of N_2 molecules (n) in small clusters of $C_6H_6(N_2)_n$ and $(N_2)_n$. The increase of cluster configurations with cluster size is roughly exponential and is larger for the inhomogeneous cluster than the homogeneous one.

The cluster configuration averaged binding energy increases nearly linearly with cluster size (n). The binding energy for C_6H_6/N_2 is much greater than that for N_2 alone: C_6H_6 thus serves as a nucleation center for N_2 condensation. Benzene as an impurity in N_2 gas will markedly accelerate nuclei formation in a condensing N_2 gas. $C_6H_6(N_2)_n$ n = 1, . . . 10 clusters have been observed in supersonic expansions[22]. In Figure 2 we present cluster binding energy as a function of the number of N_2 molecules in an $(N_2)_n$ cluster and a $C_6H_6(N_2)_n$ cluster. Note that the binding energy for a cluster is a sensitive function of cluster configuration for fixed n. Moreover, as n increases the range of binding energies also increases.

In all crystal-like N_2 clusters, as shown in Figure 3a, the distance between two closest N_2 molecules is always ca. 3.4 Å. The same is true for $C_6H_6(N_2)_n$ ($n \geq 2$) with the N_2 molecules on the same side of the aromatic ring: the N_2 molecules lie parallel to one another, as shown in Figure 3b. The N_2 molecules can thus build a similar crystal-like structure (3.4 Å separation) whether or not a benzene nucleation center is present.

The absolute value of the cluster potential energy for a given configuration decreases as the temperature of the cluster increases, until a temperature is reached at which the molecules begin to tunnel between different cluster potential wells (configurations). Although thermal motion within clusters exists at all non-zero temperatures, most of the cluster configurations are quite stable at low temperature; for example, tunneling between different configurations has not been observed for $C_6H_6(N_2)_2$ clusters in the course of ca. 10^7 MC simulations up to ca. 30 K. [Our published experimental results are consistent with these findings.[22]]

Figure 4 gives an example of such time behavior - note how small the energy fluctuations are in each well.

At a temperature for which an N_2 molecule can move between different configurational potential wells in a $C_6H_6(N_2)_2$ cluster, cluster potential energy fluctuates not only at each configuration but also between the two accessible configurations. Such behavior is displayed in Figure 5 for a $C_6H_6(N_2)_2$ cluster at 33 K. The ensemble averaged potential energy now falls between the potential energies of the two distinct "solid" or "crystalline" cluster configurations. Of course, the energy fluctuation also increases dramatically at the onset of tunneling in this example.

Cluster size increases with temperature as does the average intermolecular distance, due to a general thermal expansion. Tunneling may or may not affect this average separation for very small clusters depending on the configurations between which the tunneling occurs. Even if tunneling does affect the intermolecular distance, the standard deviation of the averaged intermolecular distances receives a large additional contribution from the tunneling process.

Solvent (N_2) molecules begin to dissociate from the cluster as the temperature is raised further. Figure 6 shows the behavior of the cluster potential energy as molecules dissociate from the cluster at the liquid-gas phase transition.

The temperature behavior of a number of cluster properties (potential energy, intermolecular distance, and an angular displacement) and their variances are displayed in Figure 7 for the $C_6H_6(N_2)_2$ cluster system. In this study the temperature varies from 8 to 41 K at which point the clusters dissociate. Temperature behavior of the cluster is determined in the range 32 to 41 K by first preventing tunneling and then allowing it to occur in separate simulations. The system properties are therefore those averaged between these two configurations in the latter temperature range. Oscillation of the system between the cluster symmetric and asymmetric configurations generates an almost discontinuous change in some of the system properties and thus mimics a bulk liquid-solid phase transition. In this cluster system the "phase behavior" is evidenced by the potential energy and intermolecular distance; the chosen angular variable would evidence a phase transition only for the asymmetric cluster.

Similar calculations are carried out for the $C_6H_6(Ar)_1$ and $(N_2)_1$ clusters and are summarized in Figures 8 and 9. In these clusters, however, the almost discontinuous behavior appears in the angular variable.

In all of the above temperature studies the "ensemble averaged" values of the cluster properties in the tunneling region are not quite equilibrium ones due to an insufficient number of MC simulations.

IV. DISCUSSION

One of the important issues for cluster computer studies as well as experimental studies in the past years has been occurrence of phase transitions in clusters. In this section we will focus a good deal of attention on the phase behavior of the small clusters discussed in the last section as revealed by MC simulations of cluster properties and their temperature dependences. The topics addressed below are as follows: 1. Cluster properties through which phase transition phenomena can be observed and how changes in these properties relate to phase transitions; 2. definition of phase transition in small clusters; 3. structure/property relations in small clusters; and 4. structure/phase transition relations in small clusters.

A. Observation of Phase Transitions

Phase transitions in small clusters have been suggested based on the results of both simulations and experiments[1-3,9-16,23]. We address in these few paragraphs those cluster properties through which liquid-solid phase transitions may be detected.

The temperature behavior of the cluster internal potential energy, intermolecular distances, radial distributions and their fluctuations has been employed to characterize cluster phase transitions. These properties can be directly obtained through MC simulations; their fluctuations are given in a canonical ensemble as

$$\sigma_E^2 = \langle E - \langle E \rangle \rangle^2 = \langle E^2 \rangle - \langle E \rangle^2$$

$$= kT\left(\frac{\partial \langle E \rangle}{\partial T}\right)_{N,V} = kT^2 C_V. \qquad (1)$$

If the kinetic energy of a cluster is only a function of temperature, E in eq (1) is the potential energy and σ^2 is its squared standard deviation or variance. Discontinuities in σ imply discontinuities in the cluster heat capacity. Since

$$\left(\frac{\partial \Delta A}{\partial T}\right)_V = \frac{\Delta A - \Delta E}{T} = -\Delta S$$

and,

$$\left(\frac{\partial \Delta S}{\partial T}\right)_V = C_V, \qquad (2)$$

a discontinuity in E implies a first order phase transition and a discontinuity in C_V implies a second order phase transition.

A similar argument may also be constructed for the intermolecular distances:

$$\sigma_R^2 = \langle R - \langle R \rangle \rangle^2 = \langle R^2 \rangle - \langle R \rangle^2, \qquad (3)$$

and the diffusion coefficient is then

$$D = \frac{1}{6}\left(\frac{d\langle r^2(t) \rangle}{dt}\right) \qquad (4)$$

with

$$\langle r^2(t) \rangle = \{\Sigma[r(t_o + t) - r(t_o)]^2\}/\Delta t \ .$$

In equations (3) and (4), R is the intermolecular distance, r is the position of each molecule, t is time, and Δt is the time interval. If the center of mass of the cluster is taken to be the solute center, then $\sigma_R^2 = \langle r^2(t) \rangle$ for small time intervals. A discontinuous change in the intermolecular

distances with temperature results in a similar change in S and thus generates a first order phase transition. A discontinuous charge in the variance of intermolecular distance with temperature results in a similar change in the diffusion constant and thus generates a second order plane transition.

Other system properties and thermodynamic variables may also be employed to monitor phase behavior.[12] As is well known from mean field, Landau, and critical phenomena theory in general,[24] not all system variables evidence phase transition behavior with equal clarity or even equal intensity:[25,26] phase transitions are evidenced by some variables and not at all by others. One must always search for a proper property or identify an "order parameter" for a particular phase transition. The order parameter for a system phase transition can be any mode or variable η for which $\langle\eta\rangle = 0$ in the high symmetry phase and $\langle\eta\rangle \neq 0$ in the low symmetry phase. The change in the slope of $\langle\eta\rangle$ occurs discontinuously at the phase transition point (T_C, P_C, etc.). Examples of such behavior in small clusters are presented below.

B. Nature of Cluster Phase Transitions.

Homogeneous and inhomogeneous cluster structures appear to be separable into two general types: crystalline and glassy. These general qualitative and somewhat subjective categories have roughly the same meaning for clusters as they do for bulk solids.[24] Crystalline solids are thermodynamically stable (lower free energy) in a given temperature range and glassy or amorphous materials are always meta stable (higher free energy) with regard to some crystalline phase(s). These distinctions are more difficult to draw for inhomogeneous (two component) clusters than for homogeneous (one component) clusters, and for small clusters than for large ones.

At low temperature the various calculated cluster structures are stable and no tunneling between stable configurations is found for long MC or MD time scales. As the temperature is raised for MC and MD calculations, tunneling begins to occur between some and then all of the local potential energy minima (crystalline). This tunneling between cluster potential energy minima is, in our view, the onset of liquid like behavior in

the clusters; that is, the time scale behavior and the magnitude of the cluster thermal motions in an MC or MD calculation reveals phase of the cluster. Tunneling between crystalline and/or amorphous local potential energy minima is the characteristic property of the liquid state and defines the liquid range. Two temperatures consistent with these ideas can be identified: a lower temperature T_f below which all clusters are fixed in a given potential minimum and no tunneling occurs; and a higher temperature T_m above which all clusters are rapidly tunneling on the calculational time scale. The latter situation represents the liquid state for the cluster system. Partial tunneling between two or a few potential minima in a restricted space of the cluster can represent solid-solid phase transition behavior rather than a solid-liquid phase transition.

According to the above discussion, the $C_6H_6(N_2)_2$ cluster is in the liquid state as the cluster potential energy alternates between the two minimum energy structures. We assume this is the normal liquid state behavior in the MC simulation.

C Detection of Phase Transition

The observation of phase transitions in both bulk matter and clusters rests on finding the appropriate essential variable or property (i.e., order parameter) for the particular transition of concern.

Figures 5 and 7 show that the $C_6H_6(N_2)_2$ cluster has two distinct "crystalline" structures with different potential energies. When the cluster is in either potential energy state the cluster energy and its fluctuation and the cluster intermolecular distance and its fluctuation both vary smoothly with temperature. When the cluster begins to tunnel between these two configurations the cluster potential energy is the ensemble average of the two different configurational potential energies. The cluster is then said to be in the liquid state and a (solid-liquid) phase transition is assumed to have occurred. The fluctuation in cluster potential energy also receives an extra contribution through this tunneling process and the fluctuation or standard deviation of the potential energy, the heat capacity, can also evidence a phase transition. Due to the number of available potential energy minima or other details of a cluster system, the potential energy function might not show a discontinuity but its variance might. The

transition would thereby be characterized as second order. Similar behavior can be found for the intermolecular distance. In general, if a cluster has two or more potential wells, a phase transition (of some order) and an appropriate property or order parameter can be found for it.

Phase transitions have been studied previously by both MC and MD simulation techniques.[1-3,9-12] The work of ref. 2 suggests that the MD results show a phase transition but that the MC results do not (Figure 10a) for the particular potential form given in Figure 10b. This discrepancy was explained as follows: in the microcanonical ensemble (MD simulation) near the melting temperature the potential is nonergodic but in the canonical ensemble (MC simulation) the potential is ergodic. Thus the system ensemble average MD properties would not be equal to the time averages of these properties. We suggest an alternative explanation. In a MD simulation, particles move continuously according to the classical laws of motion: a particle sees all walls or abrupt changes in the potential surface. In a MC simulation the phase space of the system is sampled randomly: particles more finite differences discontinuously or not at all, in the commonly applied fast coverage Metropolis MC method. Particles in a MC simulation would thereby be blind to an infinitely thin wall as used in the potential shown in Figure 10b and the actual potential experienced by a particle in a MC simulation would thus be like that in Figure 10c. The MD and MC results are different because the MD potential is a double well potential with a thin wall and the MC potential is a single well step potential.

If a cluster has numerous but identical potential wells, the temperature behavior of the potential energy and its variance will not evidence a solid-solid or solid-liquid phase transition. Consider $C_6H_6(N_2)_1$ or $(Ar)_1$ with two identical potential energy minima above and below the plane of the benzene ring. This point is made in Figures 8a and 9a.

If a cluster has numerous potential wells for which the intermolecular distance or radial distributions are the same, the temperature behavior of the distance/radial distributions and their variances will not evidence a solid-solid or solid-liquid transition. Again this point is well made for $C_6H_6(N_2)_1$ and $(Ar)_1$ as shown in Figures 8b and 9b.

The cluster property which can be employed to monitor a solid-solid or solid-liquid phase transition in clusters such as $C_6H_6(N_2)_1$ and $C_6H_6(Ar)_1$ is the angular variable and its variance (Figures 8c and 9c). Clearly the change in the angle between the intermolecular (atomic) center line and the axis perpendicular to the benzene ring and its variances represents molecular tunneling between potential wells and may then serve as an order parameter for this type of phase transition. In order to observe a phase transition for the various possible physically meaningful clusters (or more rigorously potential energy surfaces) that might arise, the appropriate phase transition coordinate or order parameter must be identified and its temperature behavior monitored.

D. Cluster Structure and Phase Transitions

According to the above discussion, we should be able to predict the order parameter for a given cluster phase transition based on the detailed potential energy surface of the cluster. Inhomogeneous clusters tend to have more potential energy minima with different energies and shapes than do homogeneous clusters of the same size and thus energy and distance behavior would be more likely to evidence phase transitions in inhomogeneous clusters than homogeneous clusters.

Clusters that possess more than one potential well should evidence phase (solid-solid or solid-liquid) transition behavior and thus have distinguishable solid and liquid phases. Examples of such clusters would be $(N_2)_2$, $(N_2)_2Ar$, $(Ar)_4$; however, even for these clusters the potential energy as a function of temperature will not evidence the phase transition. Clusters with only one potential well should not have two different "condensed" phases. Examples of this type of cluster would include $N_2(Ar)_1$, $(Ar)_2$, and $(Ar)_3$.

E. Surface Free Energy and Nucleation.

As we have pointed out, the number of possible cluster configurations increases nearly exponentially with the size of the cluster. Most of these configurations are of an amorphous, rather than a crystal, nature. Both the binding energy/molecular and entropy/molecule increase

faster for large clusters than small ones and thus the chemical potential decreases faster for large clusters than for small ones. Molecules at the "surface" of a liquid state cluster (composed of rapidly tunneling molecules) can only flow inward to the center of the cluster and have unsaturated van der Waals intermolecular bonds. The smaller the proportion of these high energy, low entropy surface molecules a cluster has, the lower its chemical potential (free energy/molecule) will be. Of course, this explains why large clusters grow at the expense of small ones. These two factors, enthalpy/molecule and entropy/molecule, account for the so called surface free energy in the liquid drop approximation[27] for large clusters. Clearly, at low temperatures for non-tunneling solid clusters and for small clusters, the notion of surface free energy is not a useful concept.

Moreover, nucleation theory based solely on the free energy of formation of clusters should be inadequate for low temperature systems because tunneling between the many cluster configurations should be almost entirely halted and thus the clusters are not in thermodynamic equilibrium.

V. Summary and Conclusions

Numerous district cluster configurations are found for even small clusters. At low temperatures the cluster configurations are quite stable and no tunneling between them is found. Most of the solid cluster configurations in big inhomogeneous clusters correspond to the glassy solid phase; a few configurations are of a crystalline nature. Within certain temperature ranges, the solid phases begin to "melt" to the liquid phase through tunneling between configurations of different geometry and potential surfaces.

The cluster energy is roughly proportional to (n-1) and increases with cluster temperature. The cluster potential energy and its variance may show a first order or second order phase transition between solid and liquid phases if the cluster has at least two potential energy minima. At higher temperatures the liquid phase cluster can evaporate molecules. The cluster intermolecular distances and their variances may also serve as a

measure of phase transition behavior under appropriate conditions of the potential surface.

The liquid state of a cluster is characterized by fast tunneling of molecules between the various cluster potential energy minima.

If a cluster has two phases, that is, a potential surface with at least two either distinct or identical potential energy minima, a cluster thermodynamic property or order parameter can always be found which characterizes (allows one to detect and follow) the phase transition. In some instances neither potential energy nor intermolecular distances (and their variances) are proper order parameters for the predicted solid-liquid phase transition. Other order parameters such as angular distributions can be employed to detect these higher order transitions.

The macroscopic surface free energy of large (liquid drop) clusters arises from two microscopic terms: restricted molecular movement at the surface, an entropy term; and unsaturated van der Waals levels at the surface, an enthalpy term.

Based on the calculations and observations reported in this work, we can make the following three predictions: 1. the solid liquid transition temperature range will be larger for small clusters than for big ones; 2. inhomogeneous clusters will have a larger phase transition range than homogeneous clusters of the same size; and 3. clusters such as $(Ar)_{2,3,}(N_2)Ar$ have only a single phase, while $(N_2)_2$ and$(Ar)_4$ have two phases.

References

1. C. L. Birant and J. J. Burton, Nat. Phys. Sci., **243**, 100 (1973).
2. C. L. Briant and J. J. Burton, J. Chem. Phys., **63**, 2045 (1975).
3. J. Jellinek, T. L. Beck and R. S. Berry, J. Chem. Phys., **84**, 2783 (1986).
4. J. K. Lee, J. A. Barker and F. F. Abraham, J. Chem. Phys., **58**, 3166 (1973).
5. P. Cieplak, T. P. Lybrand and P. A. Kollman, J. Chem. Phys., **86**, 6393 (1987).
6. D. L. Freeman and J. D. Doll, J. Chem. Phys., **82**, 462 (1985).
7. K. S. Kim, M. Dupuis, G. C. Lie and E. Clementi, Chem. Phys. Letters, **131**, 451 (1986).
8. F. F. Abraham, J. Chem. Phys., **61**, 1221 (1974).
9. R. D. Etters and J. Kaelberer, Phys. Rev., **A11**, 1068 (1975).
10. J. B. Kaelberer and R. D. Etters, J. Chem. Phys., **66**, 3233 (1977).
11. R. D. Etters and J. Kaelberer, J. Chem. Phys., **66**, 5112 (1977).
12. N. Quirke and P. Sheng, Chem. Phys. Letters, **110**, 63 (1984).
13. H. Reiss, P. Mirabel and R. L. Whetten, J. Phys. Chem., **92**, 7241 (1988).
14. R. S. Berry, J. Jellinek and G. Natanson, Phys. Rev., **A30**, 919 (1984).
15. M. Y. Hahn and R. L. Whetten, Phys. Rev. Letters, **61**, 1190 (1988).
16. J. Bosiger and S. Leutwyler, Phys. Rev. Letters, **59**, 1895 (1987).
17. G. Nemethy, M. S. Pottle, and H. A. Scheraga, J. Phys. Chem., **87**, 1883 (1983).

18. R. F. McGuire, F. A. Momany and H. A. Scheraga, J. Phys. Chem., **76**, 375 (1972).

19. F. A. Momany, L. M. Carruthers, R. F. McGuire, and H. A. Scheraga, J. Phys. Chem., **78**, 1595 (1974).

20. Program MOPAC 5 is obtained from J. J. P. Stewart and J. A. Menapace in Frank J Seiler Research Laboratory, USAFA.

21. W. H. Press, B. P. Flannery, S. A. Teukolsky and W. T. Vetterling, ***Numerical Recipies***, (Cambridge University, 1986).

22. R. Nowak, J. A. Menapace and E. R. Bernstein, J. Chem. Phys., **89**, 1309 (1988).

23. J. Ross and R. P. Andres, Surface Sci., **106**, 11 (1981).

24. L. D. Landau and E. M. Lifshitz, ***Statistical Physics***, (Pergamon, 1970).

25. A. Yoshihara, E. R. Bernstein and J. C. Raich, J. Chem. Phys., **79**, 445 (1983).

26. A. Yoshihara, W. D. Wilber, E. R. Bernstein and J. C. Raich, J. Chem. Phys., **76**, 2064 (1982).

27. G. S. Springer, Adv. in Heat Transfer, **14**, 281 (19).

Table I

Parameters of the atom-atom L-J (6-12-1) potentials for Pairs of like atoms.[17]

atom type	designation	C_{kk} kcalÅ^6/mol	10^{-4} A_{kk} kcalÅ^{12}/mol	r_{kk} Å
H_1	aliphatic hydrogen	45.5	1.409	2.92
H_2	amide or amine hydrogen	45.5	0.842	2.68
H_3	aromatic or sulfhydryl hydrogen	45.5	1.438	2.93
H_4	hydroxyl or carboxylic acid hydrogen	45.5	1.168	2.83
C_5	tetrahedral aliphatic carbon	370.5	90.61	4.12
C_6	carbonyl, carboxylic acid, carboxylate, or peptide bond carbon	766.6	104.9	3.74
C_7	aromatic or olefinic carbon	509.5	65.36	3.70
N_8	amide or amine nitrogen	401.3	37.52	3.51
O_9	carbonyl or carboxylic acid(C=O) oxygen	369.0	17.02	3.12
O_{10}	hydroxyl, carboxylic acid (C-O-H), or ester oxygen	217.2	12.56	3.24
S_{11}	sulfur	2274.4	580.9	4.15

FIGURE CAPTIONS
MONTE CARLO SIMULATIONS OF
SMALL SOLUTE/SOLVENT CLUSTERS:
CLUSTER PROPERTIES AND PHASE TRANSITIONS

Figure 1. The number of configurations with different cluster potential energies as a function of the number of N_2 molecules (n) in the cluster: —— $C_6H_6(N_2)_n$ clusters, and ------- $(N_2)_n$ clusters, note the dramatic increase in the number of configurations with the cluster size.

FIGURE 2. Cluster binding energies as a function of cluster size for $C_6H_6(N_2)_n$ clusters and $(N_2)_n$ clusters: --- $C_6H_6(N_2)_n$ clusters and ••••• $(N_2)_n$ clusters. The vertical lines are not error bars but indicate the ranges of the binding energies for different cluster configurations. Both the binding energies and their ranges increase almost linearly with the cluster size.

Figure 3. Two configurations of the N_2 clusters: a. "crystallized" $(N_2)_6$ - distance between each near pair of N_2 molecules is about 3.4 Å; b. $C_6H_6(N_2)_4$ clusters - distance between each near pair of N_2 molecules is again about 3.4 Å.

Figure 4. Time behavior of the absolute cluster potential energy of the two $C_6H_6(N_2)_2$ cluster configurations at 4.5 K. One configuration has one N_2 molecule at each side of the benzene ring, and the other has both N_2 molecules on the same side of the benzene ring. The time scale is represented by the number of MC simulation steps. Each point on the upper curve represents 1600 MC steps and on the lower curve is 200 MC steps. As indicated on the figure, and is true at any temperature, the symmetric cluster configuration has lower potential energy. Energy fluctuations are extremely small and no interpotential well tunneling can be observed.

Figure 5. Time behavior of the absolute cluster potential energy of the $C_6H_6(N_2)_2$ cluster at 32.5 K. The cluster potential energy

fluctuates between two distinct values: one value for the configuration with one N_2 molecule at each side of the benzene ring; and the other value for the configuration with both N_2 at one side of the benzene ring. The time scale is represented by the number of MC simulation steps. Each point on the curve represents 26900 MC steps. MC step size is always adjusted to let the number of accepted moves to be roughly the same as the number of the rejected moves.

Figure 6. Time behavior of the absolute cluster potential energy of the $C_6H_6(N_2)_2$ cluster at 42 K. The cluster potential energy fluctuates between the two distinct energy levels and then decreases to zero in a stepwise fashion. This latter behavior arises because the molecules begin to dissociate from the cluster one after another. The time scale is represented by the number of MC simulation steps: each point on the curve represents 25700 MC steps.

Figure 7. The temperature behavior of the cluster a. potential energy, b. intermolecular distances c. angle θ between the intermolecular line joining the two molecular mass centers and the Z axis perpendicular to the benzene ring and their variances for $C_6H_6(N_2)_2$ clusters: both N_2 molecules at one side of the ring (solid circle); one N_2 molecule at each side of the ring (empty circle); and the statistical average of these two configurations at thermal equilibrium (cross). Tunneling between the two distinct potential wells is purposefully prohibited at higher temperatures in order to obtain the results for the two distinct configurations. The number of MC simulation steps for the points on the figure increases with temperature, in order to reduce the statistical error. At 32.0 K each point represents about 2×10^7 MC steps. Simulation is stopped above 41 K at which temperature the cluster begins to evaporate. The temperature behavior of the cluster potential energies and the intermolecular distances show a solid-liquid phase transition. (The crosses at 32K are not representative of equilibrium values due to the limited number of simulations.) The temperature behavior of the angle θ of the statistically averaged configuration overlaps with that of the configuration with one N_2 at each side of the ring.

Figure 8. The temperature behavior of the cluster potential energy, the intermolecular distance, the angle between the intermolecular line joining the two molecular mass centers and the Z axis perpendicular to the benzene ring, and their variances for the $C_6H_6(Ar)_1$ cluster. MC simulation is stopped above temperature 26 K, at which temperature the cluster begins dissociation. The temperature behavior of the cluster potential energy and the intermolecular distance show no sign of a liquid-solid phase transition; however, the temperature behavior of the angle variable clearly indicates that a phase-transition-like phenomenon occurs around 20 K.

Figure 9. The temperature behavior of the cluster a. potential energy b. the intermolecular distance, c. angle between the intermolecular line joining the two molecular mass centers and the Z axis perpendicular to the benzene ring, and their variances for the $C_6H_6(N_2)_1$ cluster. MC simulation is stopped above temperature 42 K, at which temperature the cluster begins to dissociate. See Figure 8 caption for more detail.

Figure 10. The model potential well(s) and MC and MD simulations from the work of ref 2.
a. Potential energy vs temperature for MC and MD simulation results.
b. One dimensional potential well of ref. 2 used in these calculations.
c. Potential well experienced by a particle in these MC simulations.
See text for a full explanation of these calculations and calculation dependent potentials.

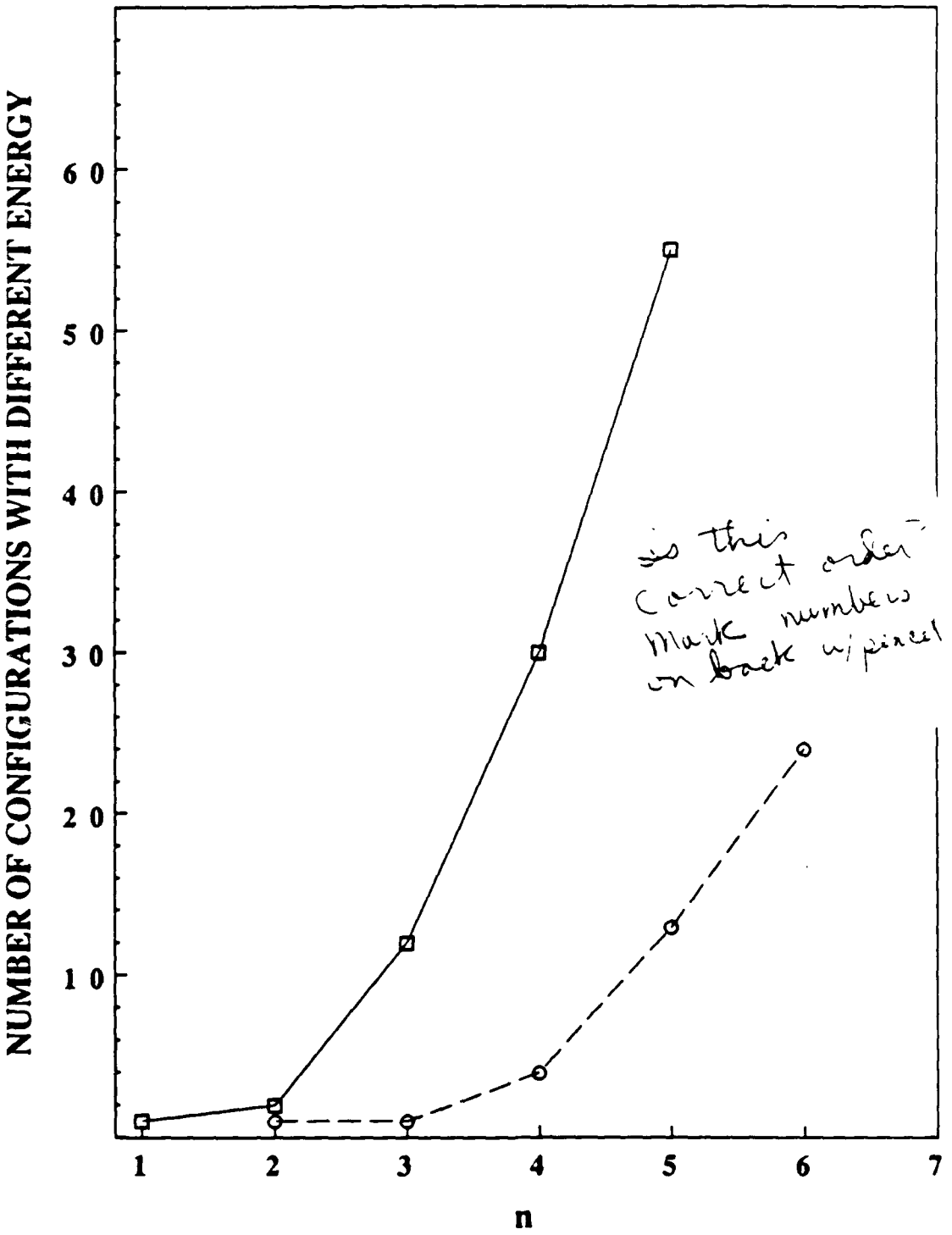
NUMBER OF CONFIGURATIONS WITH DIFFERENT ENERGY
60
50
40
30
20
10
1
2
3
4
5
6
7
n
is this correct order?
Mark numbers on back w/ pencil

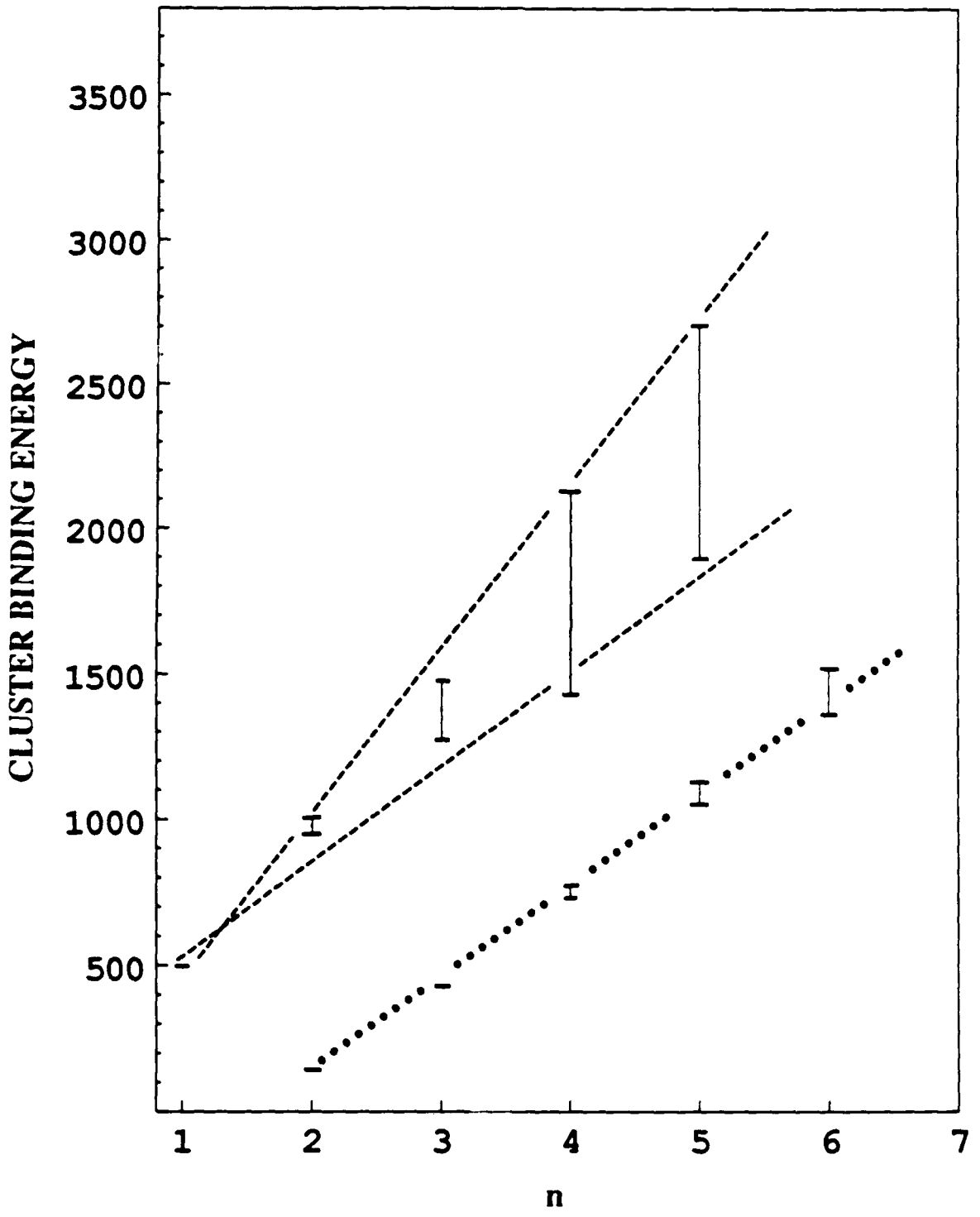
CLUSTER BINDING ENERGY
3500
3000
2500
2000
1500
1000
500
1
2
3
4
5
6
7
n

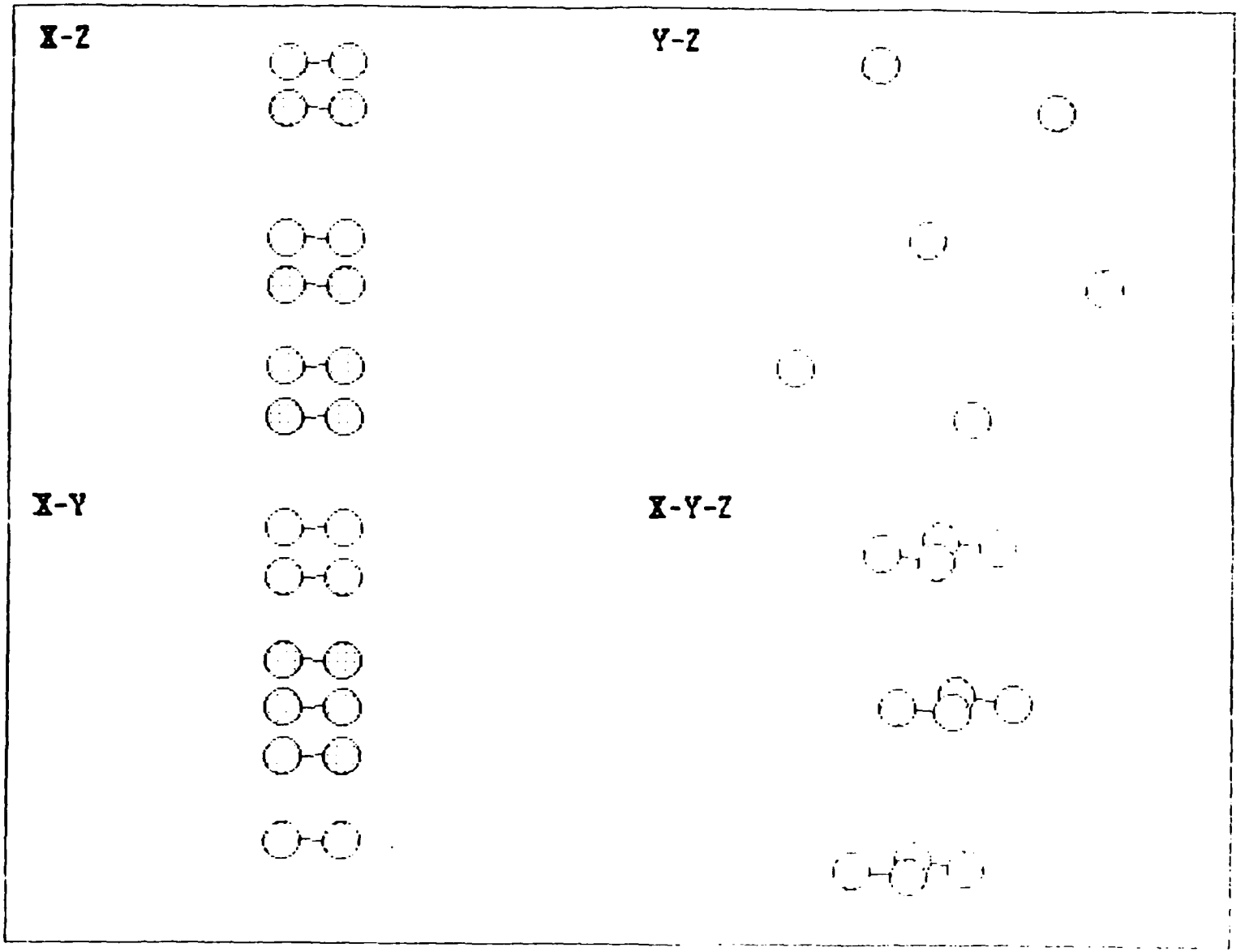
X-Z
Y-Z
X-Y
X-Y-Z

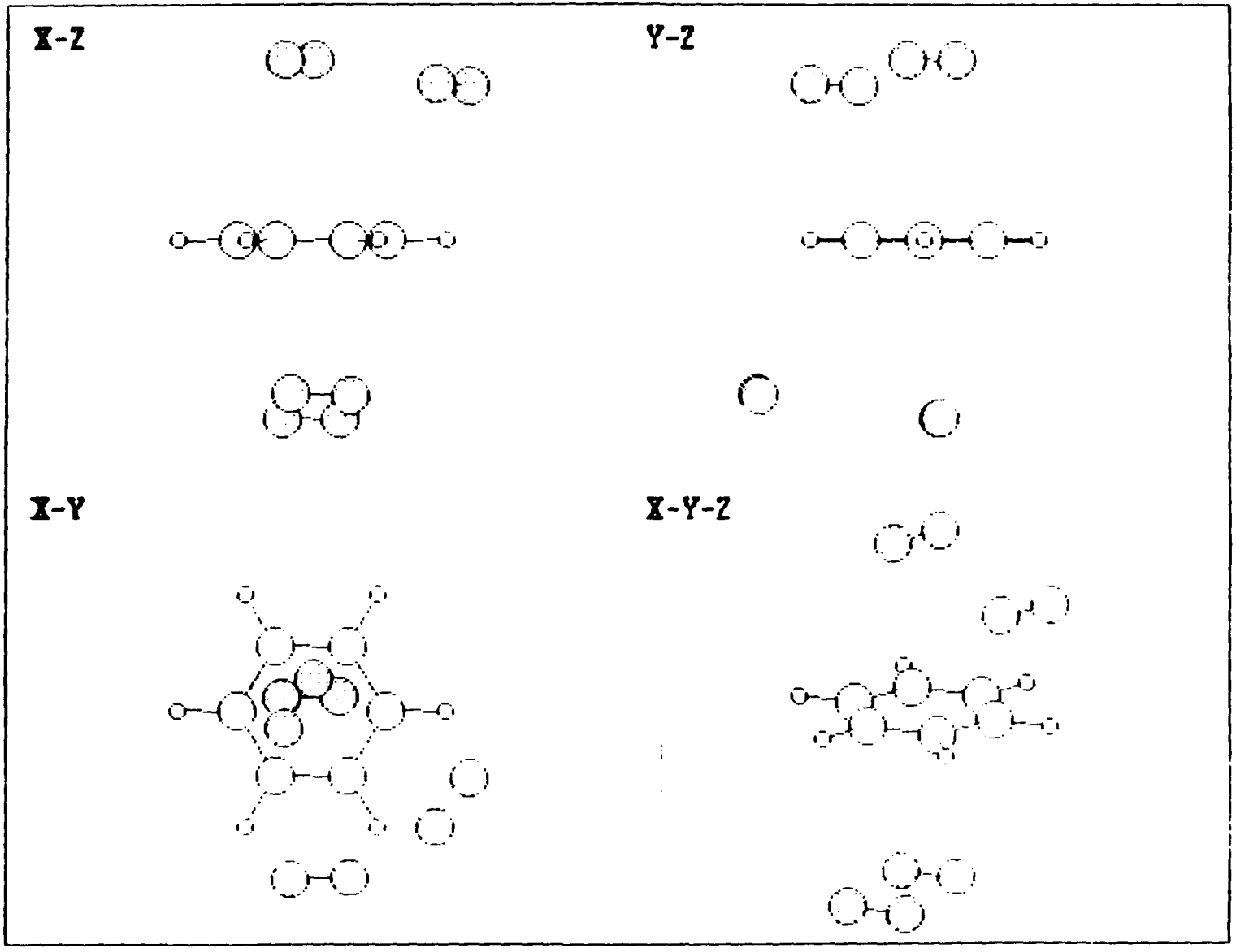
X-Z
Y-Z
X-Y
X-Y-Z

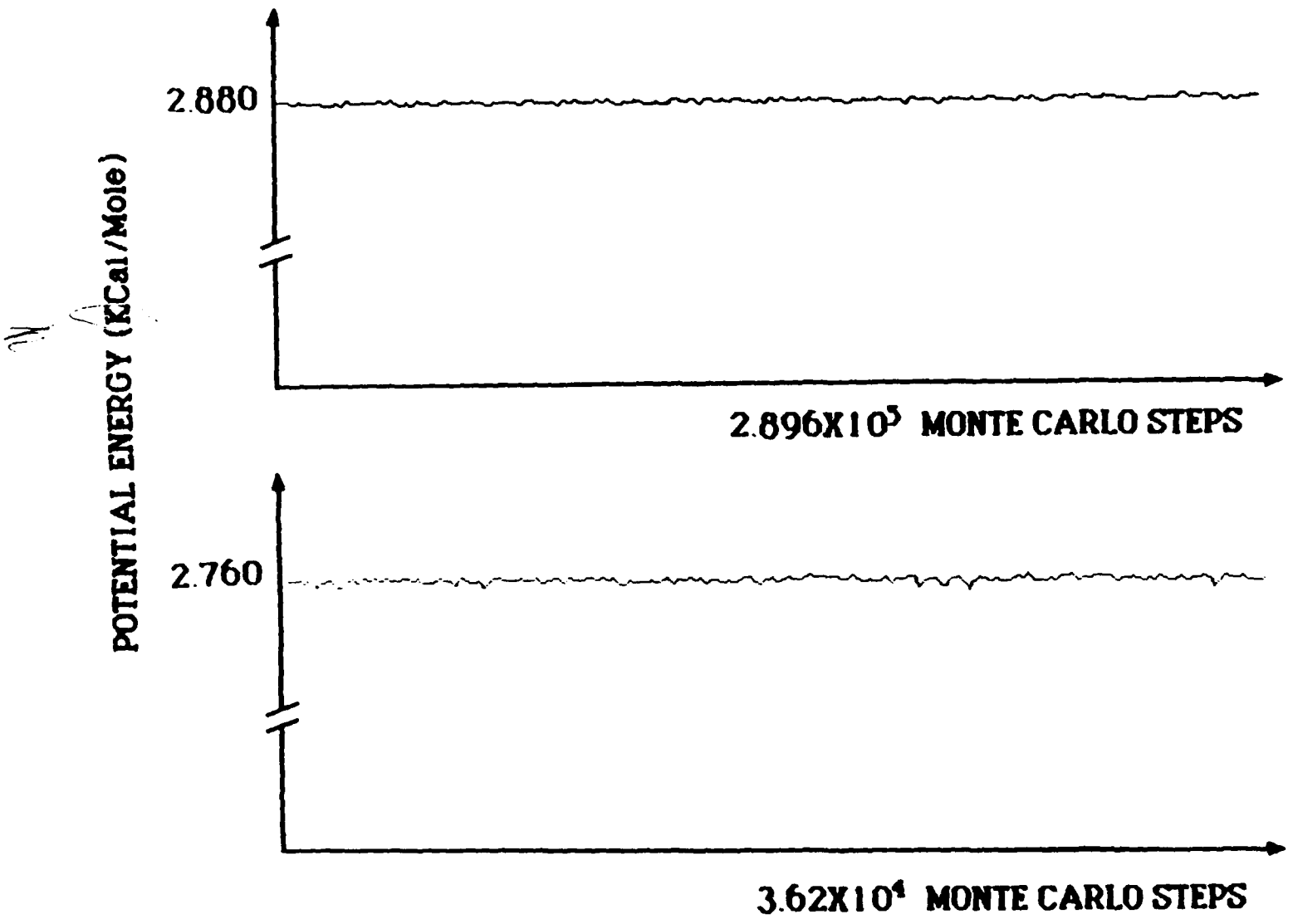
2.880
POTENTIAL ENERGY (KCal/Mole)
2.896X10^5 MONTE CARLO STEPS
2.760
3.62X10^6 MONTE CARLO STEPS

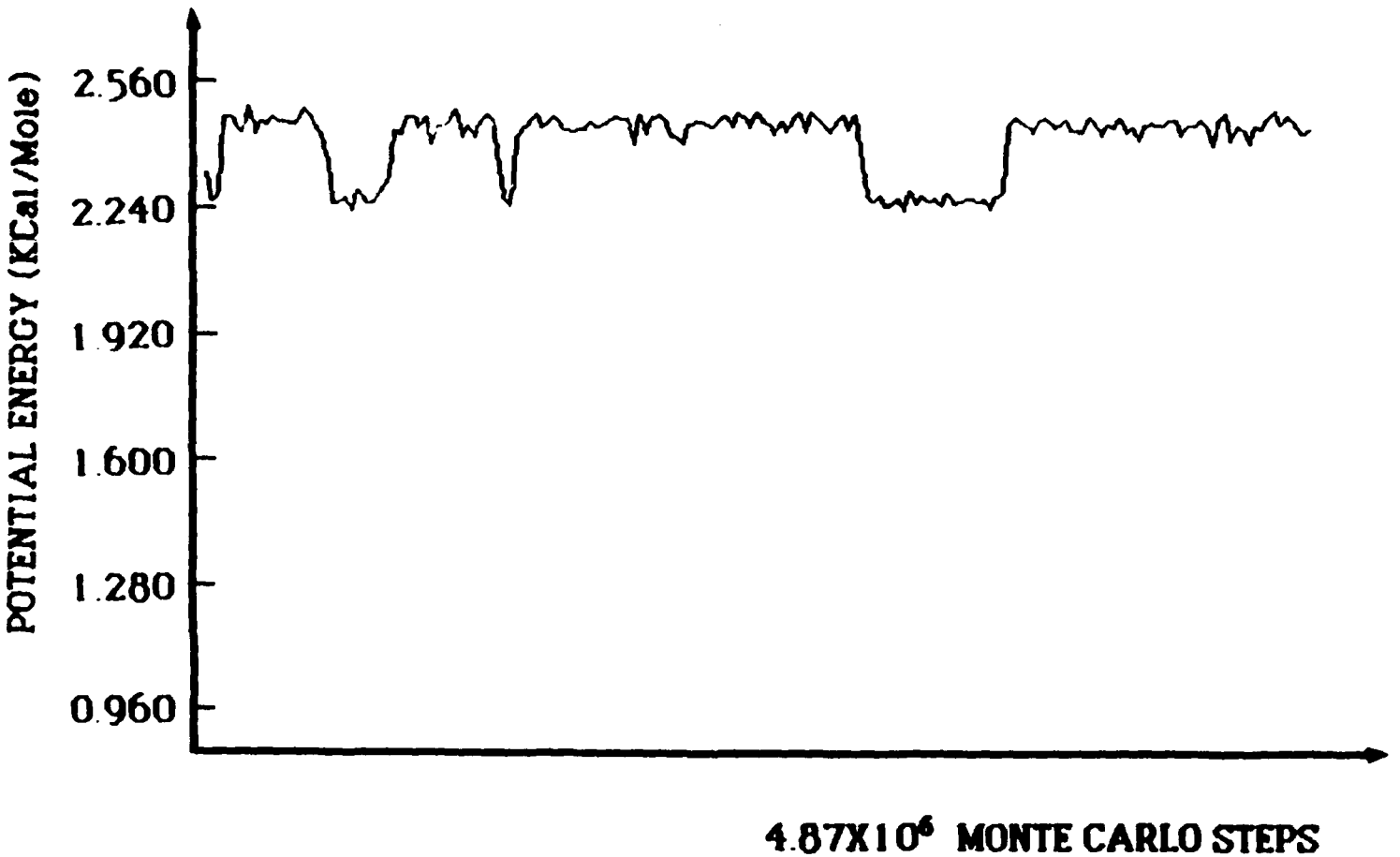
POTENTIAL ENERGY (KCal/Mole)
2.560
2.240
1.920
1.600
1.280
0.960
4.87X10⁶ MONTE CARLO STEPS

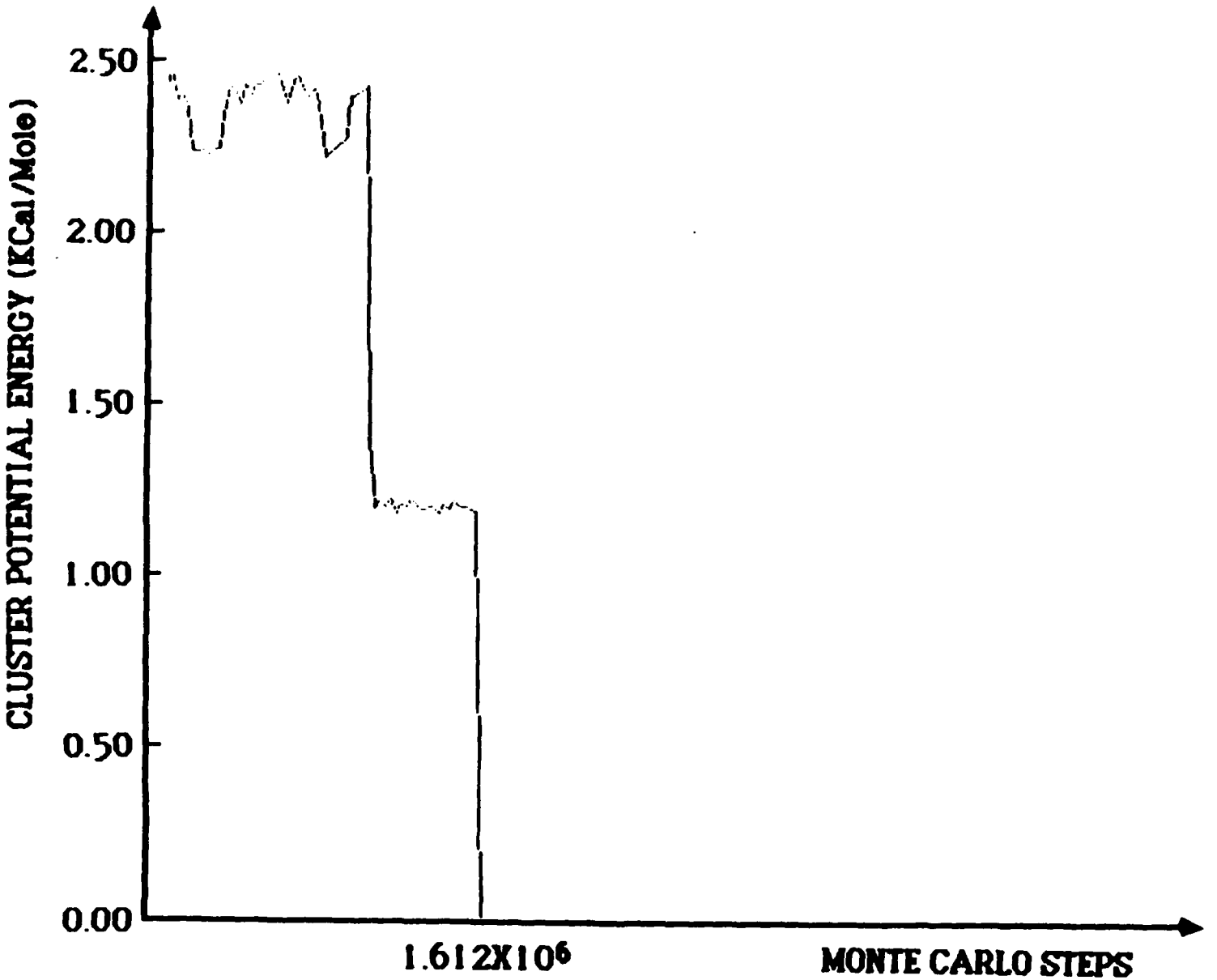
CLUSTER POTENTIAL ENERGY (KCal/Mole)
2.50
2.00
1.50
1.00
0.50
0.00
1.612X10⁶
MONTE CARLO STEPS

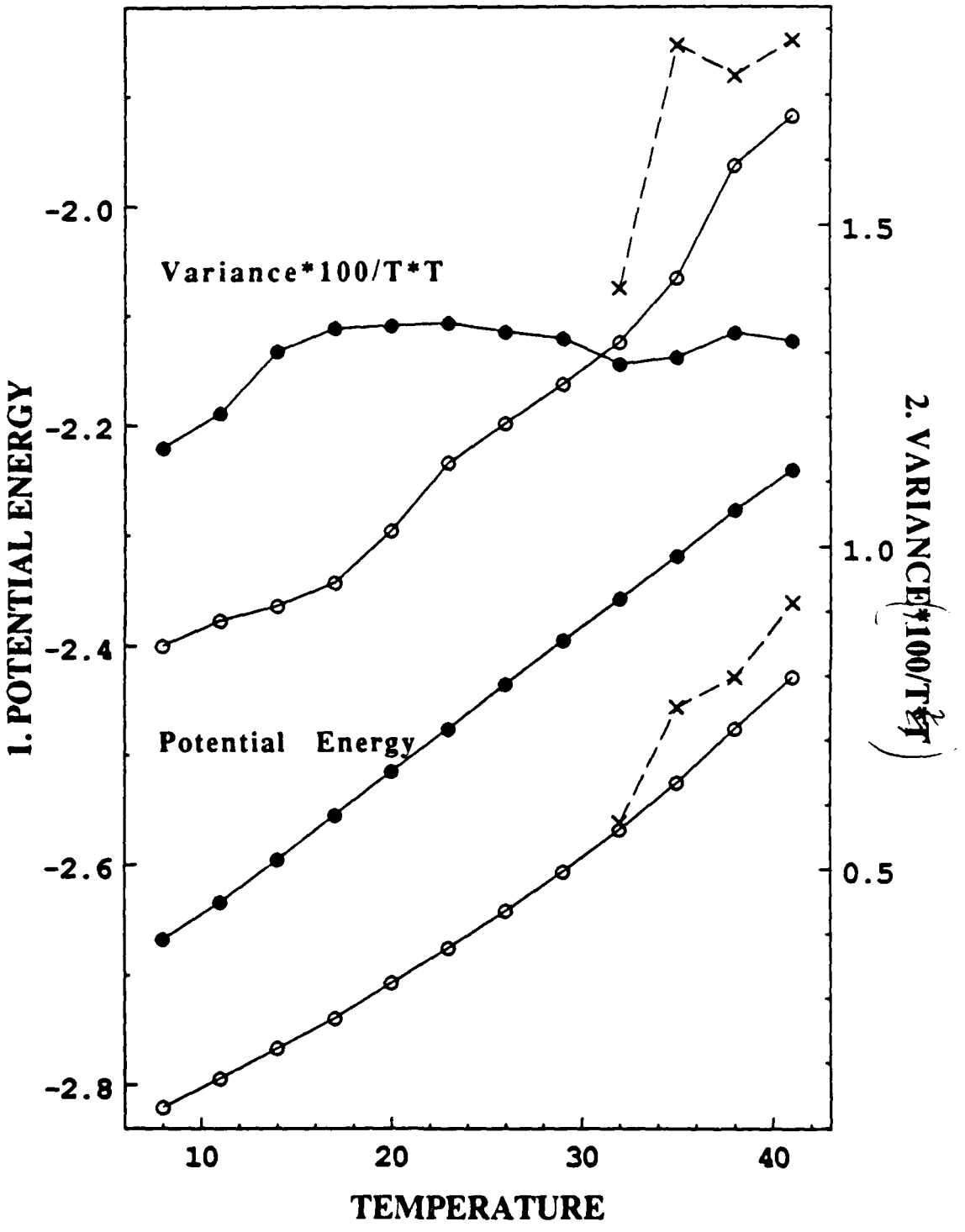
-2.0
-2.2
-2.4
-2.6
-2.8
1.5
1.0
0.5
10
20
30
40
Variance*100/T*T
Potential Energy
1. POTENTIAL ENERGY
2. VARIANCE(*100/T*T)
TEMPERATURE

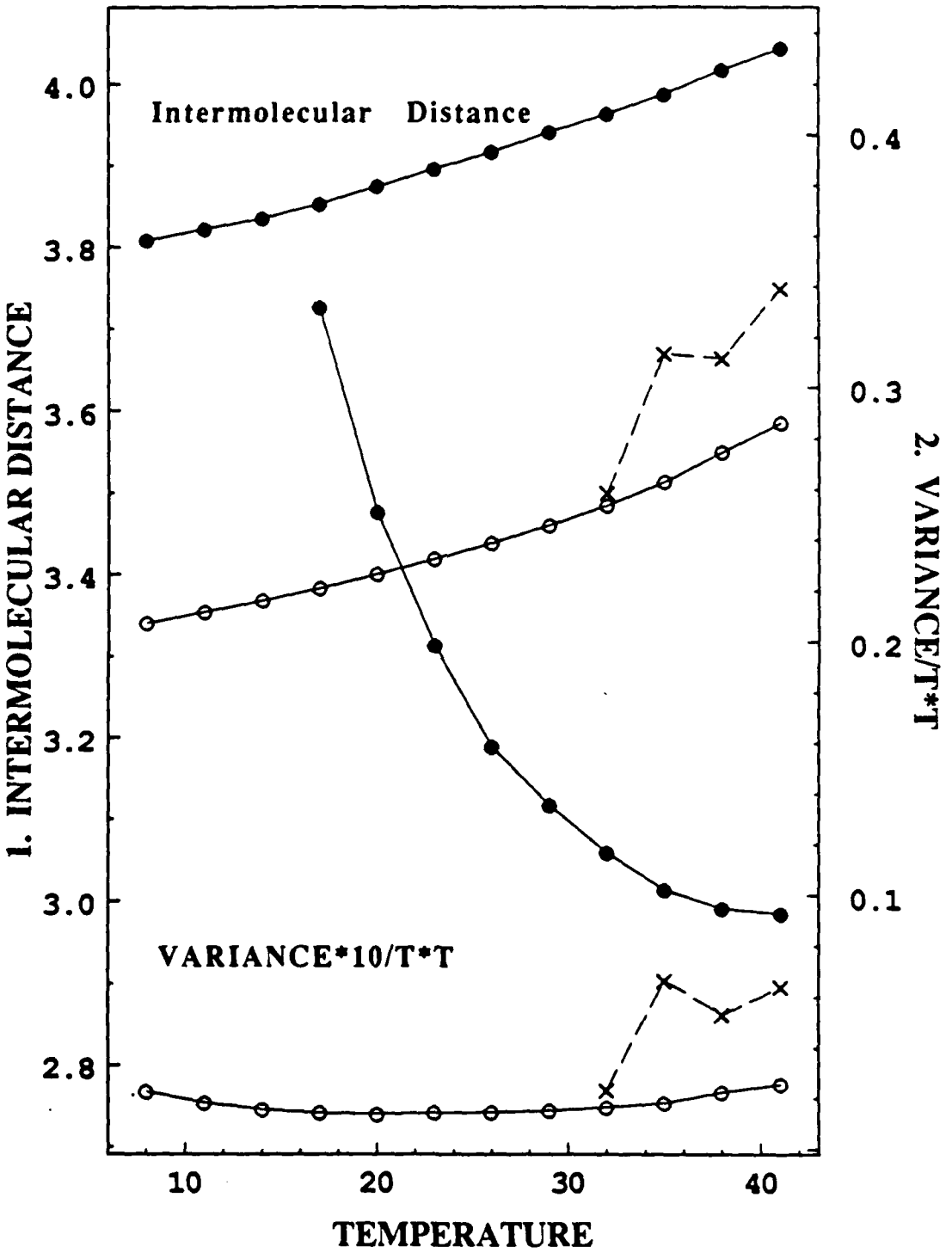
Intermolecular Distance
VARIANCE*10/T*T
1. INTERMOLECULAR DISTANCE
2. VARIANCE/T*T
TEMPERATURE
4.0
3.8
3.6
3.4
3.2
3.0
2.8
0.4
0.3
0.2
0.1
10
20
30
40

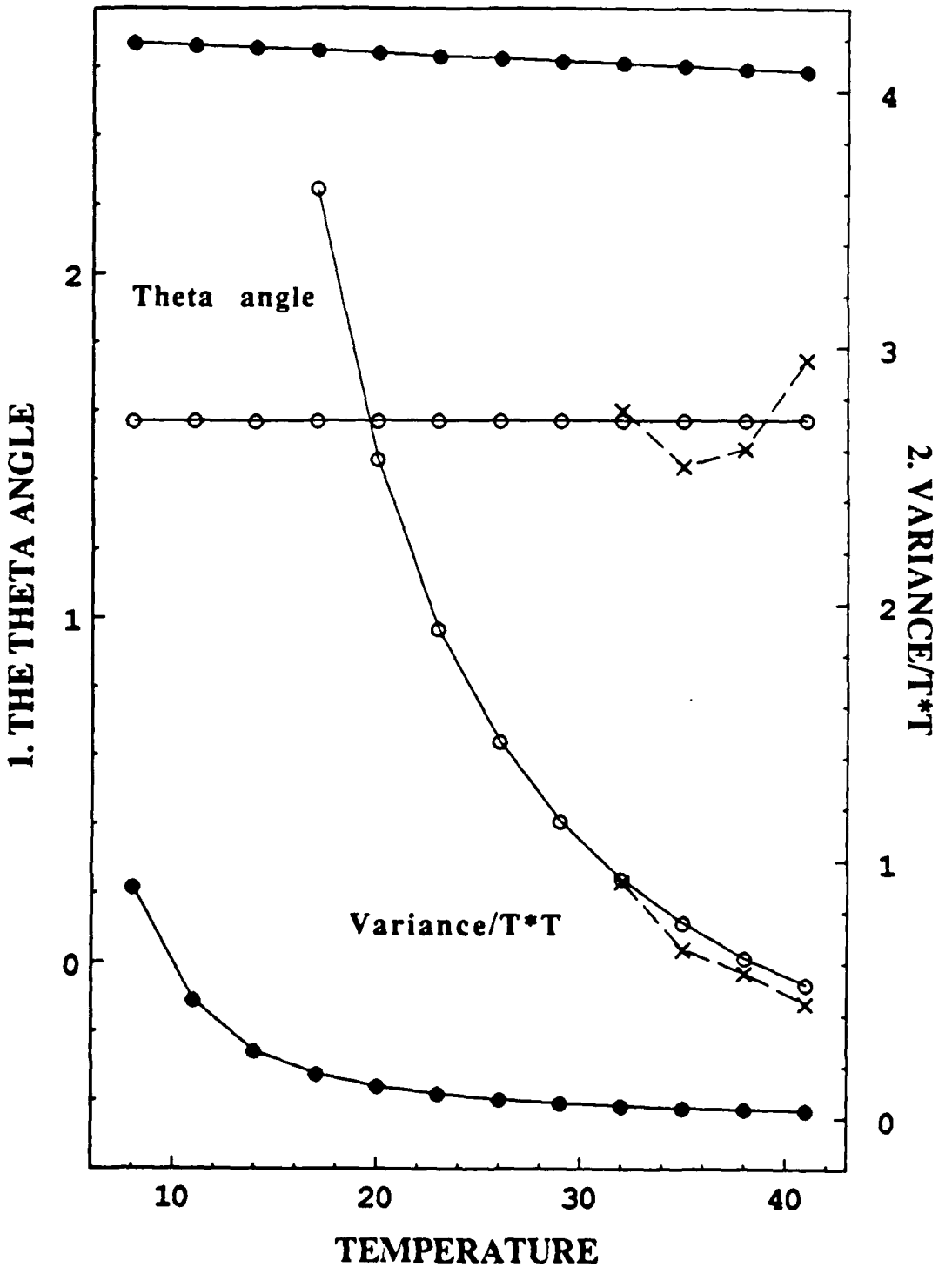
Theta angle
Variance/T*T
1. THE THETA ANGLE
2. VARIANCE/T*T
TEMPERATURE
0
1
2
0
1
2
3
4
10
20
30
40

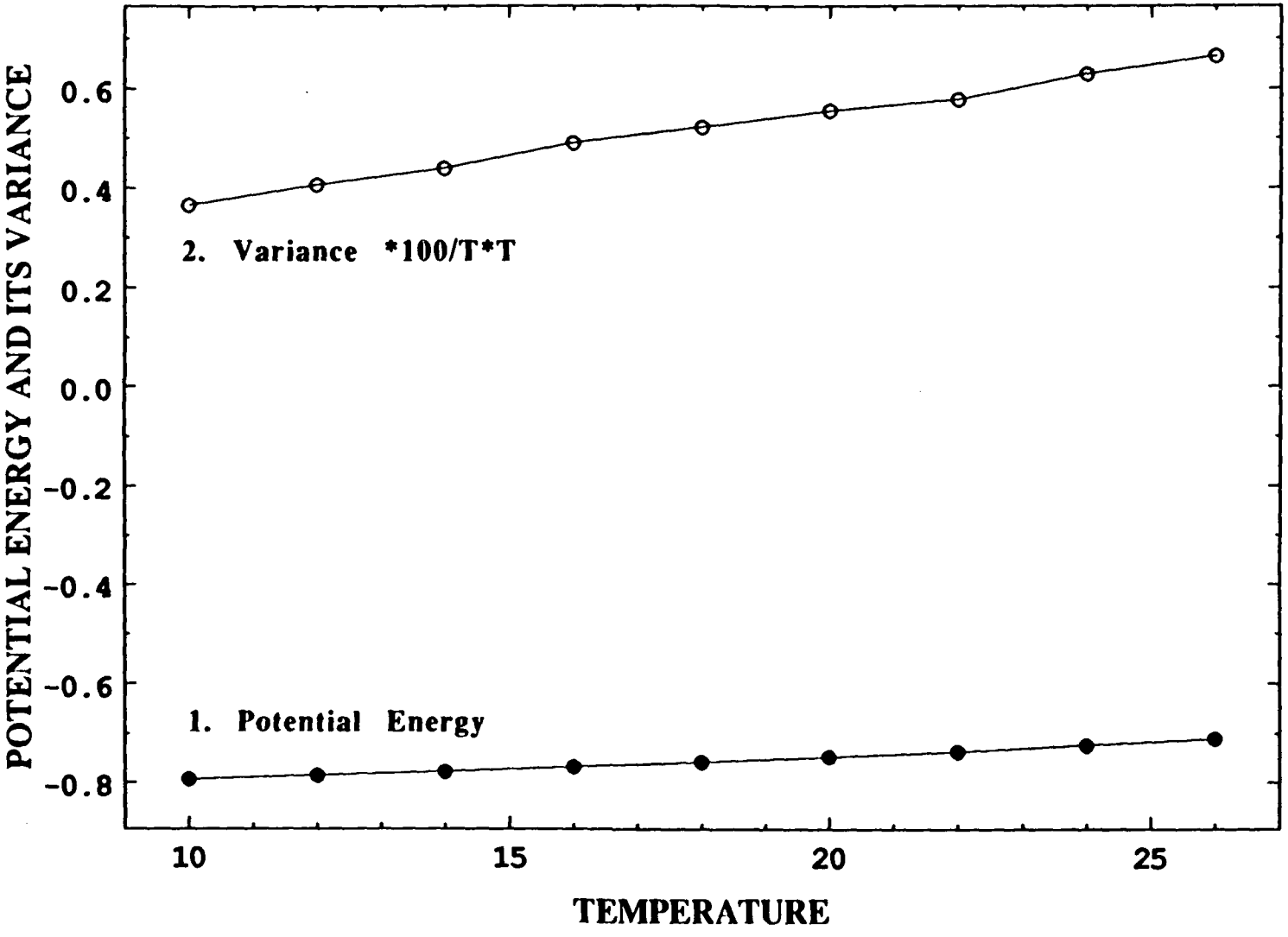
POTENTIAL ENERGY AND ITS VARIANCE
0.6
0.4
0.2
0.0
-0.2
-0.4
-0.6
-0.8
2. Variance *100/T*T
1. Potential Energy
10
15
20
25
TEMPERATURE

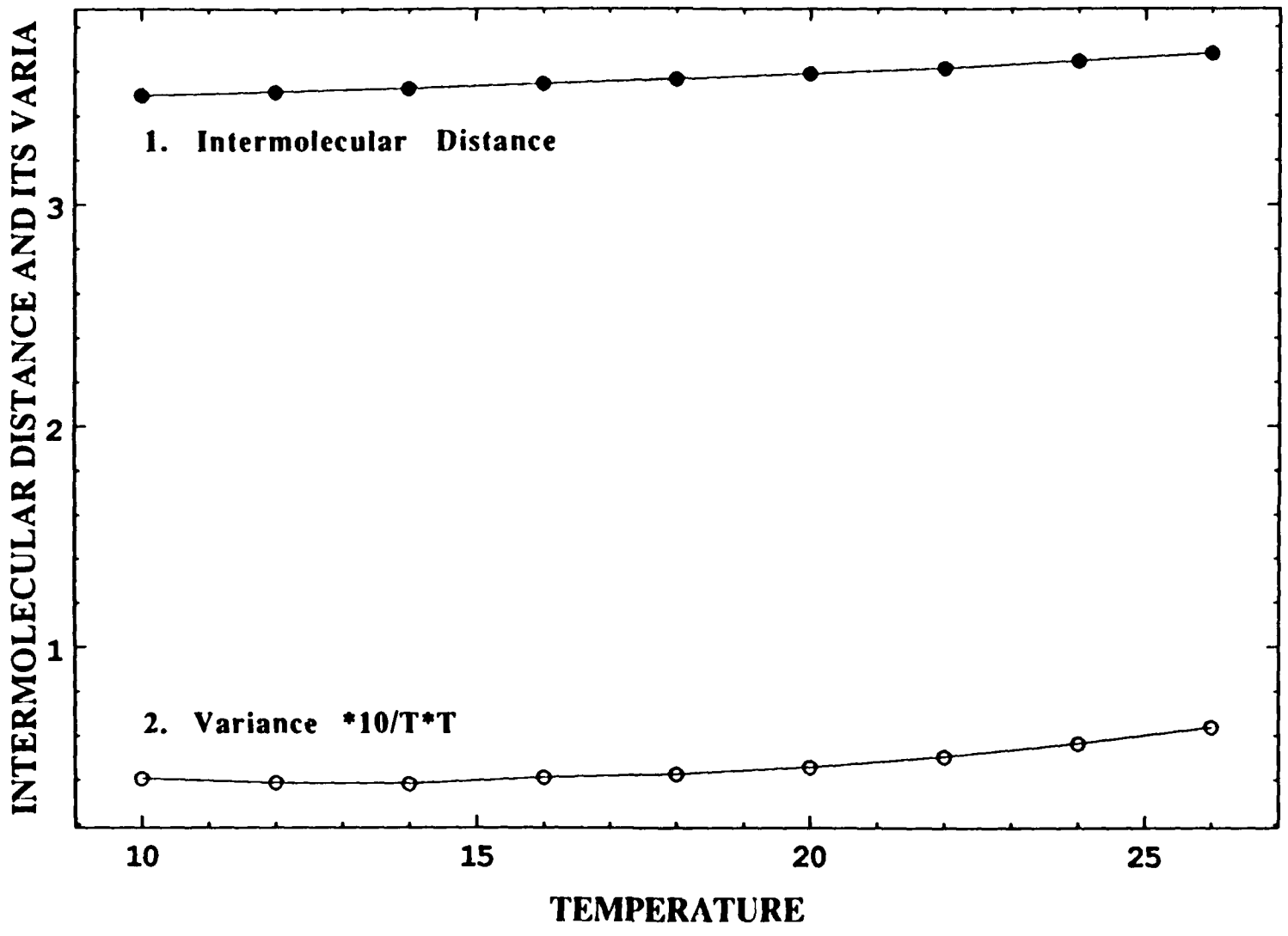
INTERMOLECULAR DISTANCE AND ITS VARIA
1. Intermolecular Distance
2. Variance *10/T*T
1
2
3
10
15
20
25
TEMPERATURE

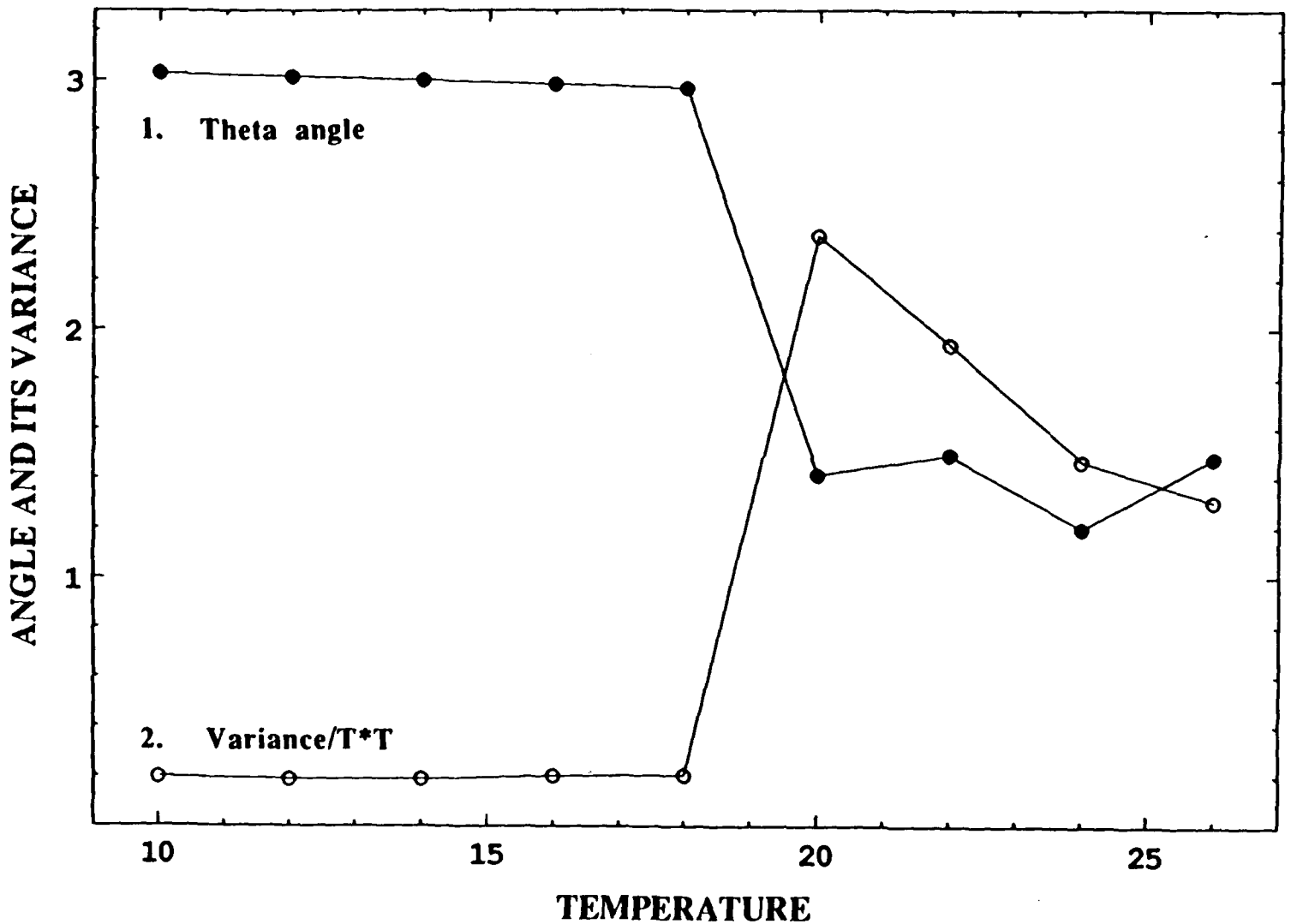
1. Theta angle
2. Variance/T*T
ANGLE AND ITS VARIANCE
TEMPERATURE
3
2
1
10
15
20
25

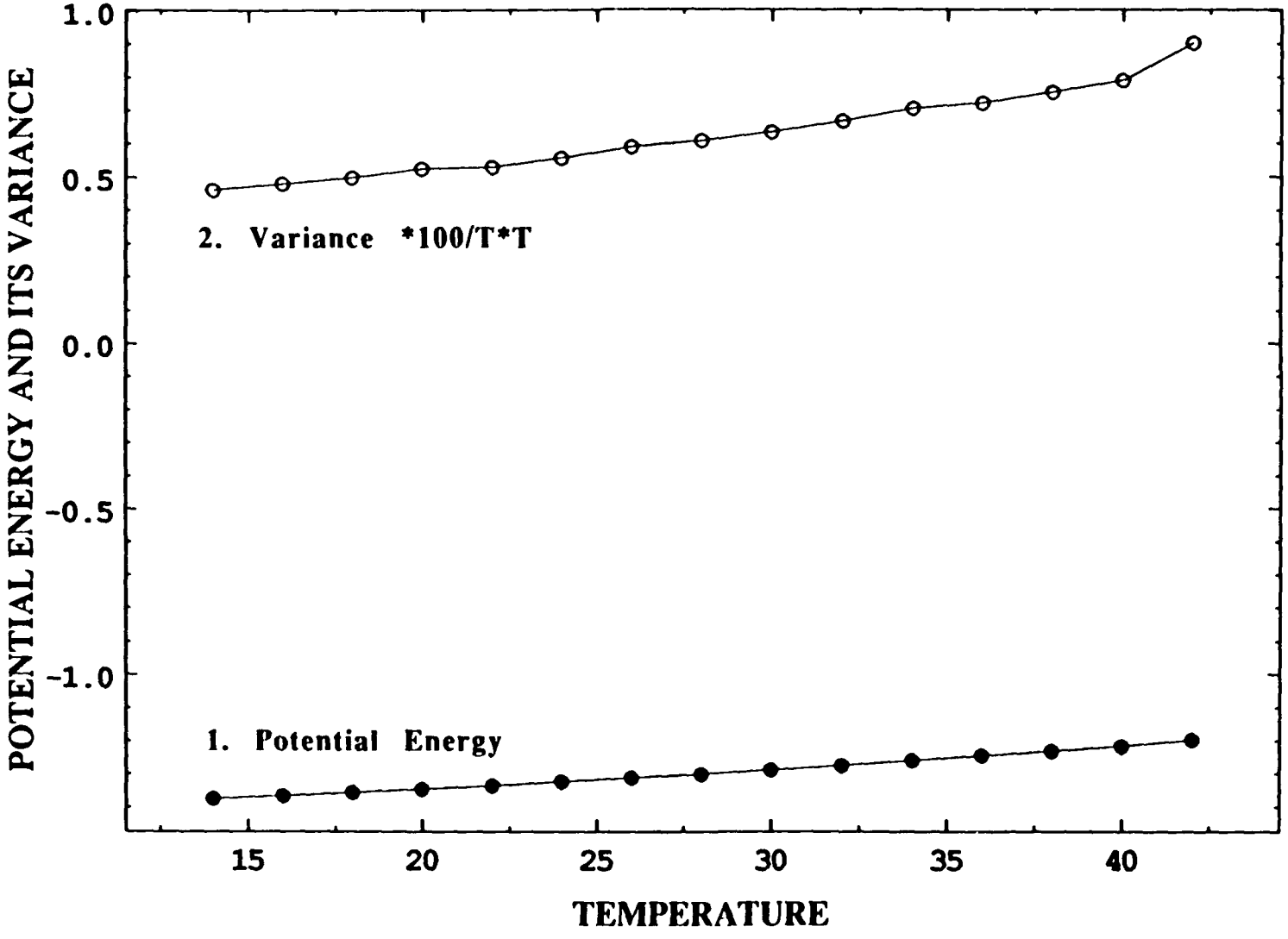
1.0
0.5
0.0
-0.5
-1.0
POTENTIAL ENERGY AND ITS VARIANCE
2. Variance *100/T*T
1. Potential Energy
15
20
25
30
35
40
TEMPERATURE

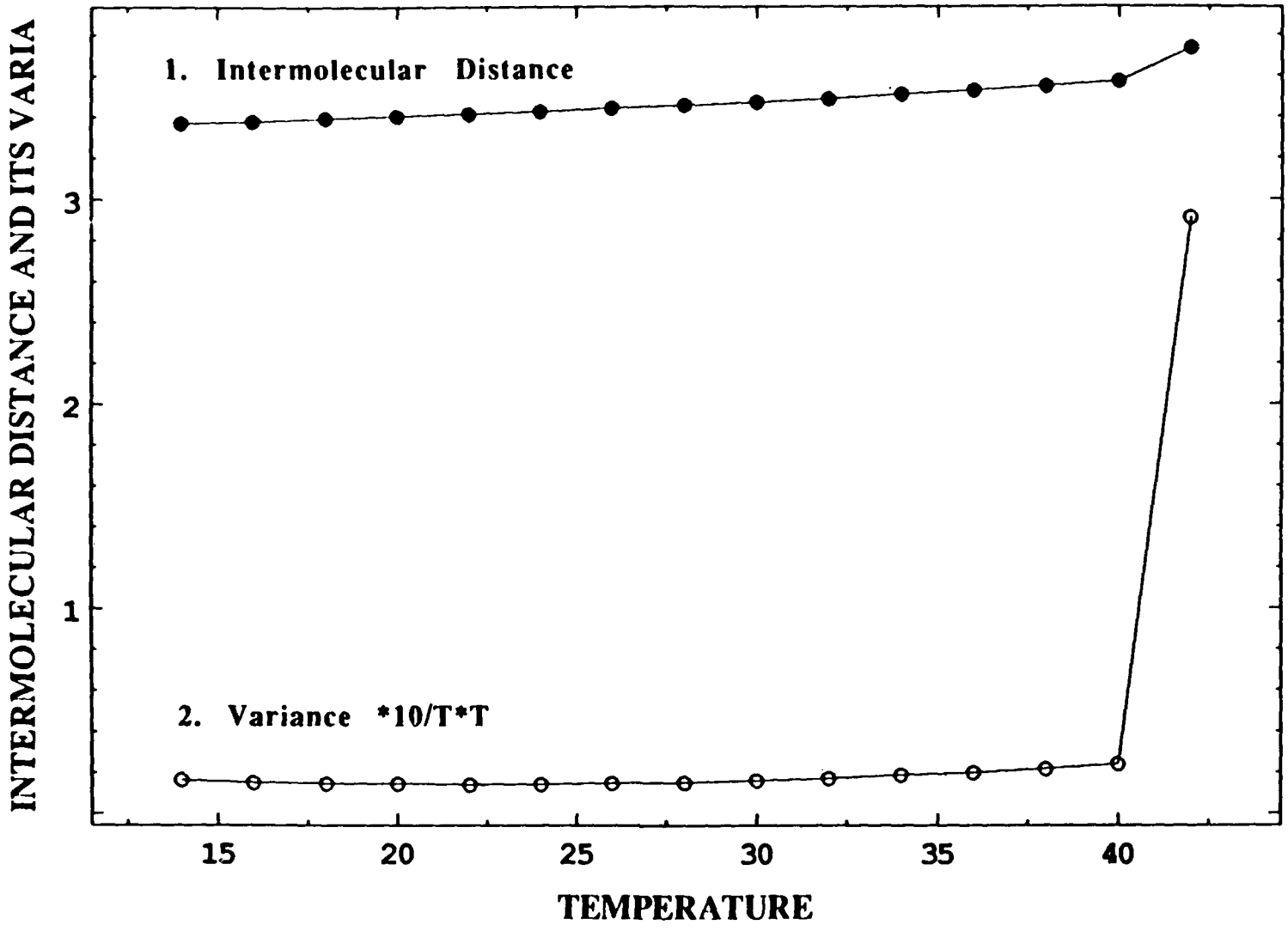
1. Intermolecular Distance
2. Variance *10/T*T
INTERMOLECULAR DISTANCE AND ITS VARIA
TEMPERATURE
1
2
3
15
20
25
30
35
40

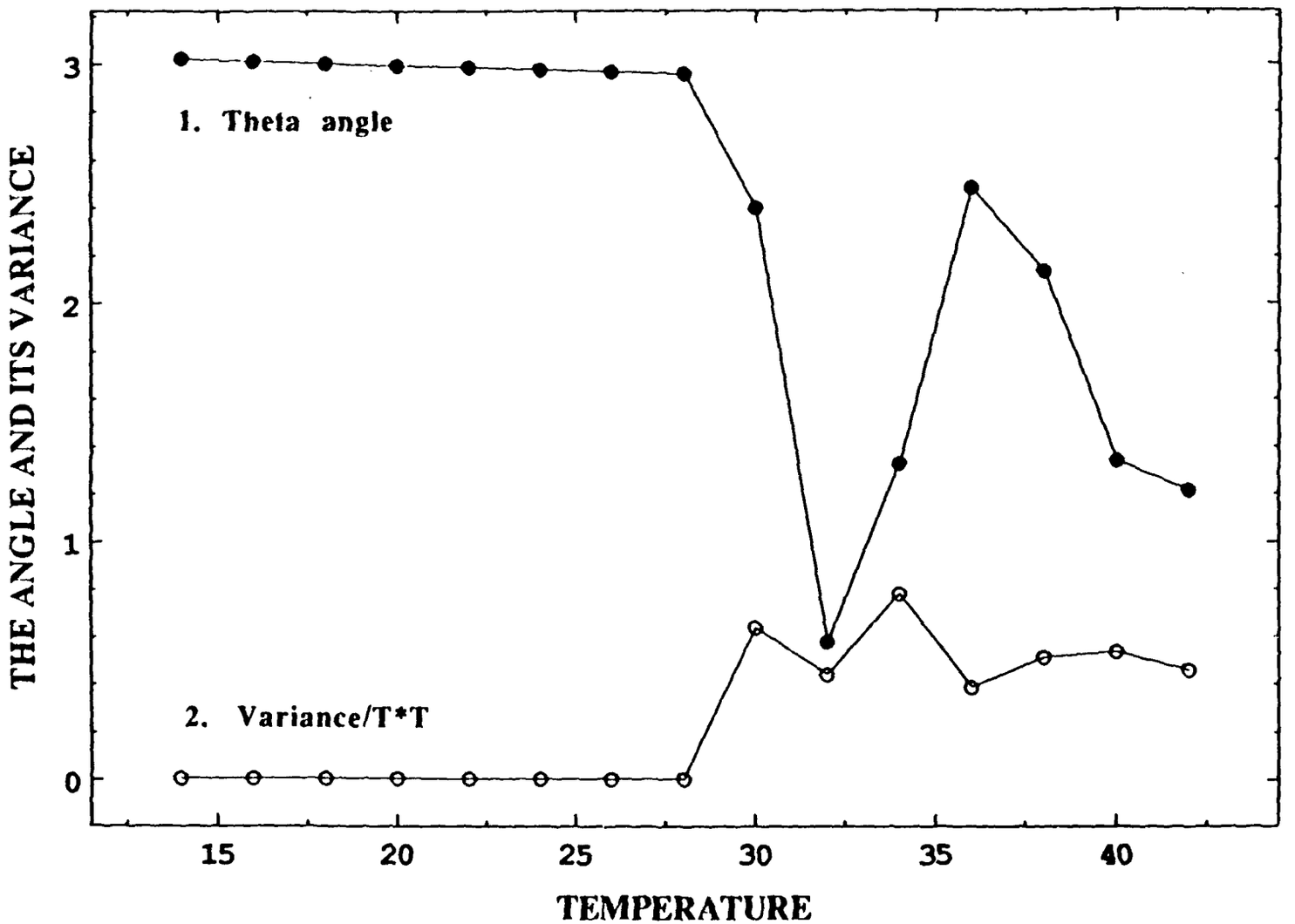
1. Theta angle
2. Variance/T*T
THE ANGLE AND ITS VARIANCE
TEMPERATURE
0
1
2
3
15
20
25
30
35
40

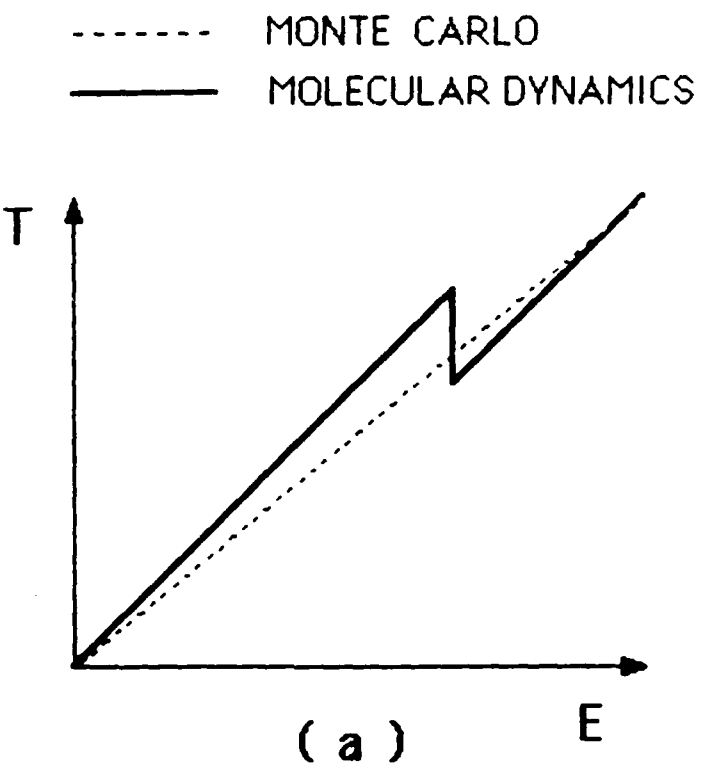

(a)

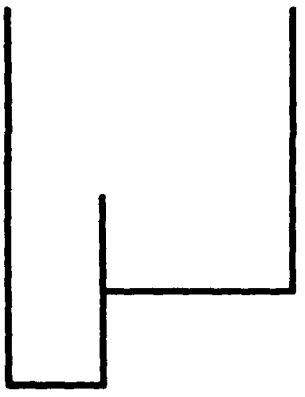

(b)

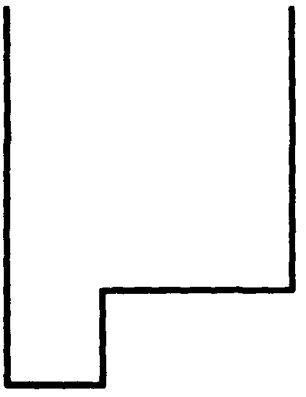

(c)

DL/1113/89/1

TECHNICAL REPORT DISTRIBUTION LIST, GENERAL

	No. Copies
Office of Naval Research Chemistry Division, Code 1113 800 North Quincy Street Arlington, VA 22217-5000	3
Commanding Officer Naval Weapons Support Center Attn: Dr. Bernard E. Douda Crane, IN 47522-5050	1
Dr. Richard W. Drisko Naval Civil Engineering Laboratory Code L52 Port Hueneme, California 93043	1
Defense Technical Information Center Building 5, Cameron Station Alexandria, Virginia 22314	2 high quality
David Taylor Research Center Dr. Eugene C. Fischer Annapolis, MD 21402-5067	1
Dr. James S. Murday Chemistry Division, Code 6100 Naval Research Laboratory Washington, D.C. 20375-5000	1
Dr. Ronald L. Atkins Chemistry Division (Code 385) Naval Weapons Center China Lake, CA 93555-6001	1
Chief of Naval Research Special Assistant for Marine Corps Matters Code 00MC 800 North Quincy Street Arlington, VA 22217-5000	1
Dr. Bernadette Eichinger Naval Ship Systems Engineering Station Code 053 Philadelphia Naval Base Philadelphia, PA 19112	1
Dr. Sachio Yamamoto Naval Ocean Systems Center Code 52 San Diego, CA 92152-5000	1
David Taylor Research Center Dr. Harold H. Singerman Annapolis, MD 21402-5067 ATTN: Code 283	1